

Diode-side-pumped Nd:YLF laser emitting at 1313 nm based on DBMC technology

Alessandro M. Deana,¹ Marcio A. P. A. Lopez,² and Niklaus U. Wetter^{2,*}

¹Universidade Nove de Julho, Rua Vergueiro 235, São Paulo (SP), Brazil

²Centro de Lasers e Aplicações, IPEN/SP, Av. Prof. Lineu Preses, 2242, São Paulo (SP), Brazil

*Corresponding author: nuwetter@ipen.br

Received May 2, 2013; revised September 11, 2013; accepted September 11, 2013;
posted September 12, 2013 (Doc. ID 189831); published October 9, 2013

Efficient lasers operating in the 1.3 μm band are of interest in the health industry for frequency conversion to the visible spectral region and for Raman shifting to the eye-safe 1.5 μm region. In this work, we demonstrate for the first time, to our knowledge, a side-pumped Nd:YLiF₄ laser emitting at 1.3 μm . An output power of up to 14.9 W was obtained at 1313 nm with 54 W of absorbed pump power, representing 27.7% optical efficiency and a slope efficiency of 45%. © 2013 Optical Society of America

OCIS codes: (140.3410) Laser resonators; (140.3530) Lasers, neodymium; (140.3580) Lasers, solid-state.

<http://dx.doi.org/10.1364/OL.38.004088>

Lasers emitting in the 1.3 μm spectral region are of interest in the health industry for cosmetic and dermatologic procedures due to the moderate absorption of the O–H molecular bond in water and because these lasers show less skin specificity due to less absorption by melanin and other pigments [1,2]. Additionally, the wavelength can be conveniently frequency-doubled and tripled to the red and blue spectral regions and Raman-shifted to the eye-safe 1.5 μm region for applications in LIDAR, range-finding, and free-space optical communication [3]. This very efficient and stable Raman conversion scheme, using four-level neodymium lasers emitting at 1.3 μm , is an interesting option, especially for high-energy pulsed laser operation, when compared with other high-power, solid-state lasers sources at 1.5 μm such as the three-level erbium laser [4]. All these applications would benefit from a small, low-cost but high-power laser source with characteristics, such as high beam quality and reduced complexity.

Efficient laser action of the $^4F_{3/2} \rightarrow ^4I_{13/2}$ neodymium transition has been obtained in several different hosts, such as YAG, GdVO₄, and YVO₄ [5–7]. The Nd:YLiF₄ (Nd:YLF) crystal presents several very interesting features for pulsed laser operation at these wavelengths, such as long upper laser level lifetime, allowing efficient energy extraction under Q-switched operation, and natural birefringence [8]. For high repetition rates and continuous wave operation, the weak thermal lensing that occurs in consequence of a negative refractive index shift with increasing temperature combined with a positive end face bulging originated from the thermally induced stress is another advantage of this host matrix [9]. The birefringence produces two different laser lines at 1321 and 1313 nm that are polarized parallel (π) and perpendicular (σ) to the c-axis of the host, respectively.

The s of the host, respective the higher emission cross-section and shows efficient laser action in a longitudinally pumped laser cavity, resulting in 3.6 W of continuous wave operation under direct pumping into the $^4F_{3/2}$ energy level at 880 nm with 7.3 W of pump power, which corresponds to 49% of optical-to-optical conversion efficiency. When pumping the $^4F_{3/2}$ level at 806 nm, the optical-to-optical efficiency and maximum output power decreased to

34% and 3.51 W, respectively [10]. The σ -polarized laser emission (1313 nm) was obtained with 6.2 W of output power and 35% of optical-to-optical efficiency when pumping at 806 nm, and under direct pumping at 880 nm, 3.1 W of output power could be achieved, corresponding to 36% optical-to-optical efficiency [11,12].

In this work, we report for the first time, to our knowledge, a side-pumped Nd:YLF laser, based on the double-beam mode-controlling (DBMC) technique [13–16], that operates in the TEM₀₀ mode. Two pump wavelengths were compared, namely, 797 and 792 nm.

In an active medium with high absorption, such as Nd:YVO₄, a single grazing incidence of a highly elliptical laser beam resulting in total internal reflection (TIR) at the pump surface is capable of efficiently screening the inverted population, thereby producing a laser with near-quantum defect efficiency [17]. However, due to the lower absorption cross-section of Nd:YLF, a single bounce results in multimode operation for pump powers little above threshold [18]. Therefore, side-pumped Nd:YLF resonators require multiple passes through the crystal, usually with elliptical beams, to achieve efficiency during fundamental mode operation. The TEM₀₀ mode itself can then be guaranteed by using some sort of hard aperture, which has the side effect of reducing the maximum output power in the fundamental mode by roughly 20% when compared with multimode operation without the aperture [19].

Different from the above method, DBMC technology creates a *soft aperture* based on the gain competition between two near-parallel laser beams inside the crystal to guarantee TEM₀₀ mode operation at high pump powers [14,18,20]. A direct proof of this soft aperture is that DBMC has achieved higher efficiencies operating in the fundamental mode than any technique has achieved in multimode operation [16]. An additional advantage is that DBMC does not need cylindrical intracavity optics to create the highly elliptical beams necessary in other techniques to screen the inverted population [17,19].

Figure 1 shows the DBMC setup: the intracavity laser beam has two TIR bounces at the pump surface. The incidence angle Φ and the separation D between the two beams are adjusted such that the overlap efficiency with

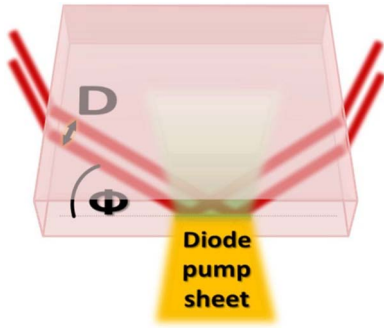


Fig. 1. DBMC setup showing both beams with separation D inside the crystal undergoing TIR at the surface.

the pump inversion is maximized and the higher order mode oscillation is prevented up to the highest pump power. The importance of correctly adjusting D is also demonstrated in [16].

It has been shown analytically that in a side-pumped resonator, which uses a single grazing incidence laser beam path at the pump surface, the threshold of the fundamental mode is always smaller than the threshold of the next higher mode [18]. This can be explained by the fact that the TEM_{00} mode has a higher power density at its center, when compared with other modes and therefore, also receives the highest pump inversion upon TIR, when the center is exposed directly at the pump surface. However, in order to achieve efficient overlap with pump inversion in gain media that have absorption length of the order of 1 mm or more, such as Nd:YLF, a much larger angle instead of a grazing angle is preferred. Our simulations have shown that a simple square-shaped crystal without antireflection (AR) coating (laser beam entrance and exit at Brewster angle) can provide the correct angle Φ and separation D for a highly efficient overlap and higher order mode suppression [16]. In Nd:YLF, the angle Φ for σ -polarization is 34.6 deg (refractive index of 1.45), which is much larger than the grazing incidence used by Damzen and co-workers [17]. However, as shown in Fig. 2, although the angle is not grazing in our

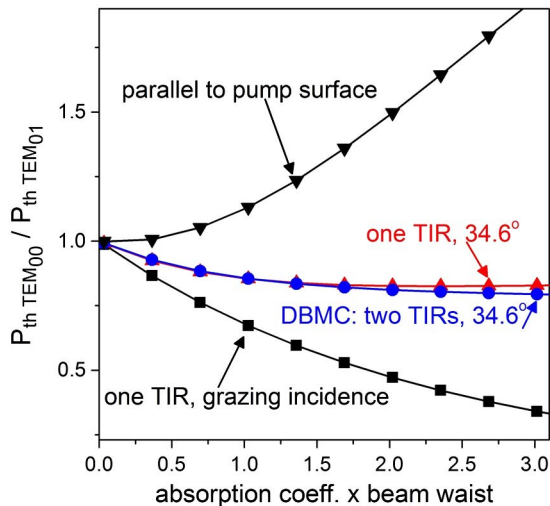


Fig. 2. Threshold of TEM_{00} divided by the threshold of TEM_{01} as a function of absorption coefficient times laser beam waist, $\alpha \times w$.

crystals, the fundamental mode still has the lower threshold and therefore, the TEM_{00} mode oscillation is guaranteed close to threshold. The lower curve in Fig. 2 is for one TIR with very small grazing incidence as in [14]. The two curves in the middle are for one or two beams with TIR at a 34.6 deg grazing angle and the upper curve is for a beam passing parallel to the pump surface at 1 mm distance. Curves with values above one as a function of $\alpha \times w$ are multimode at threshold.

Even if the laser starts to oscillate at threshold in the fundamental mode, there is still the possibility that it may change to multimode soon after the threshold. Figure 3 shows the importance of the second beam in DBMC. The simulations were done for an Nd:YLF laser operating at 1313 nm with one (left graph) and two beams (right graph). For the sake of clarity, we used in the simulation a $\alpha \times w$ product of 1.3 (see Fig. 2), which corresponds to a smaller beam size ($w = 430 \mu\text{m}$) than used actually in our experimental setup [$w = 510 \mu\text{m}$ in Fig. 4(a)]. In both cases, the laser starts to oscillate in the TEM_{00} mode (straight line in Fig. 3) at approximately 14 W of pump power. However, for one single beam (left graph), the laser becomes multimode at 16 W of pump power (arrow). From this point on, the TEM_{01} mode (dashed line) starts to oscillate. For comparison, when using DBMC (right graph), TEM_{01} joins TEM_{00} oscillation at a much higher pump power of 34 W when using a spacing D (Fig. 1) of 1 mm (for $w = 510 \mu\text{m}$ the lines cross at 67 W of pump power).

The laser setup is shown in Fig. 4(a). M1 is a plane output coupler with 90% reflectivity at 1313 nm. All mirrors have low reflectivity in the 1.06 μm region. M2 is a concave, highly reflective (HR) mirror with an 8 m radius of curvature. M3 is an HR plane mirror at 1313 nm. The 60 W fast-axis collimated pump diode was focused into the crystal by a single $f = 20$ mm spherical lens (SL). The diode's wavelength was adjusted by temperature controlling to match the 797 and 792 nm absorption peaks of Nd:YLF as shown in Fig. 4(b). Pump pulse duration and duty cycle were 1 ms and 5%, respectively, in all cases.

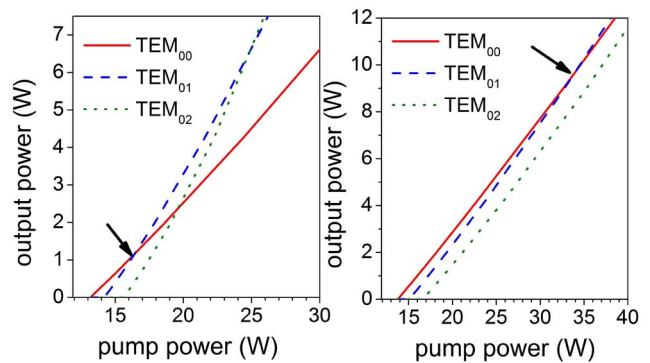


Fig. 3. Simulation of the transition from TEM_{00} mode operation to multimode operation shown in an input–output power diagram for one single beam (left) and two beams (right). The arrows indicate the pump power at which the laser starts to become multimode. The simulation only serves to show the pump power at which the laser becomes multimode and if the next rectangular transverse mode to operate has (TEM_{02}) or does not have (TEM_{01}) a central lobe.

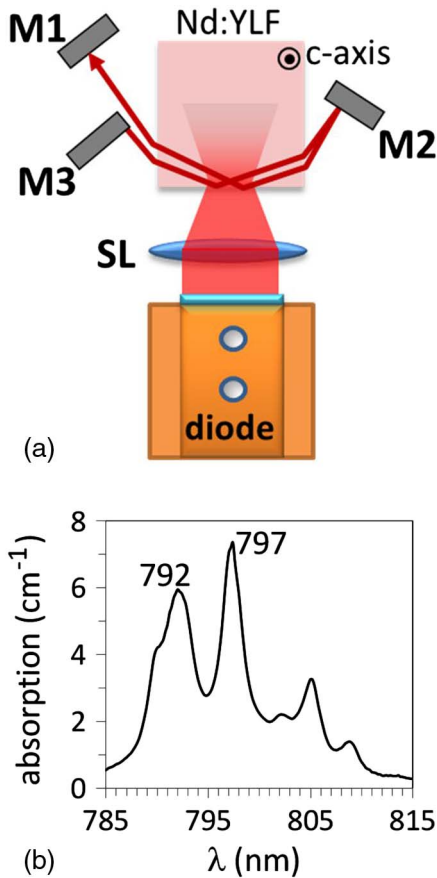


Fig. 4. Schematic diagram of (a) the laser resonator and (b) the π -polarized absorption spectrum of the 1 mol. % Nd:YLF crystal.

The resonator round-trip losses were approximately 3% as determined by means of a Findlay–Clay analysis.

The gain crystal was square shaped with dimensions of 13 mm \times 13 mm \times 3 mm, a-cut, with c -axis orientation parallel to the diode's TE-polarized emission. The peak absorption coefficient at 792 nm ($^4I_{9/2} \rightarrow ^4F_{5/2} + ^2H_{9/2}$ transition) is lower than that at 797 nm ($^4I_{9/2} \rightarrow ^4F_{5/2}$ transition), but due to its proximity with the $^4H_{9/2}$ level, the $^4I_{9/2} \rightarrow ^4F_{5/2} + ^2H_{9/2}$ transition suffers inhomogeneous broadening of its spectrum, as shown in Fig. 4(b).

Figure 5 shows output power as a function of absorbed pump power for both pump wavelengths of 797 and 792 nm. Coupling losses due to lens and nonexistent

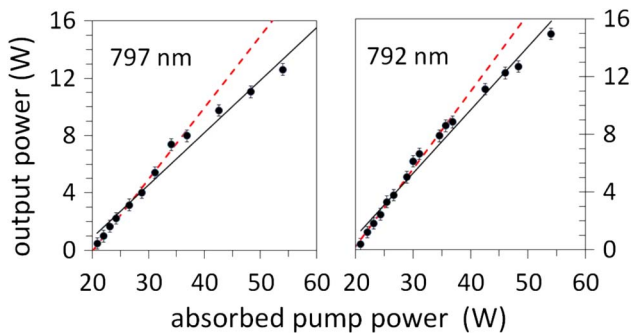


Fig. 5. Output power versus absorbed pump power for pumping at 792 and 797 nm.

AR-coating on pump facet were approximately 4.5%. For a maximum pump power of 54 W at 797 nm, 12.6 W of output power were obtained at 1313 nm, resulting in an optical-to-optical efficiency of 23.4%. The slope efficiency and laser pump threshold are 0.40 (straight line) and 19 W, respectively. By pumping at 792 nm, 14.9 W of peak output power were obtained at 1313 nm, resulting in an optical-to-optical efficiency of 27.7%. The slope efficiency and laser threshold are 0.45 and 18 W, respectively.

Figure 5 also shows a gradual roll-over of the output power, especially when pumping at 797 nm, even in the absence of a significant heat load. Regression analysis showed that the experimental data were not described properly by a linear model. The reason for the observed roll-over of the output power for pump powers beyond 40 W is a spectral broadening of the diode's emission, which increases FWHM approximately 26% when increasing the pump current from 40 to 60 A. In an end-pumped resonator scheme, overlap with the pump inversion is guaranteed due to the colinearity of the pump and the laser beam. Therefore, if the wavelength of the pump and the laser beam suffers a small shift or broadening, the overlap integral between pump inversion and the laser beam remains approximately the same, although the effective absorption coefficient decreases. In side-pumped resonators, effective absorption coefficient, intracavity laser beam cross-section, and position have to be perfectly matched for efficient operation. Any shift in the pump's spectral width strongly decreases overlap and therefore, output power. This is further enhanced by the narrow linewidth feature of the $^4I_{9/2} \rightarrow ^4F_{5/2}$ transition in Nd:YLF.

Despite the fact that 792 nm is less absorbed directly at the crystal's surface when compared with 797 nm, a higher efficiency is obtained in Fig. 5 due to the wider bandwidth of this absorption line, which matches better with the broad emission of the diode. The fact that there is less roll-over with 792 nm demonstrates that laser performance is not impacted by thermal effects at the low duty cycles employed in this experiment, but by diode broadening. This is also demonstrated by the good beam quality shown in Fig. 6 and is obtained by the knife-edge method. We measured a beam quality factor of $M^2 = 1.04$ and 1.17, respectively, along the vertical and the horizontal axis at the maximum employed pump power (54 W).

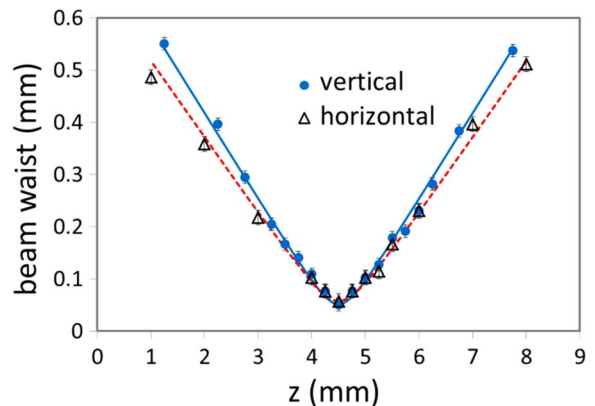


Fig. 6. Beam quality measurement of the 1313 nm beam using the 797 nm pump diode.

DBMC has been tested in Nd:YLF at higher average pump powers up to 16.5 W without deterioration of laser beam quality or slope efficiency using the ${}^4F_{3/2} \rightarrow {}^4I_{9/2}$ neodymium transition [18]. Upon increasing the average power in the Nd:YLF crystal further, fracture occurs, without a noticeable transition or roll-over in the laser output power caused by thermal lensing [15]. Beam quality changes only very slightly and the ${}^{TEM}_{00}$ mode is maintained until fracture [15].

Considering in Fig. 5 the slope of the output power curve for 792 and 797 nm (dotted lines) from threshold to 40 W of pump power (this is before diode spectral broadening sets in), the slope efficiencies are 54% and 50%, respectively, and the optical-to-optical conversion efficiency at the maximum available absorbed pump power of 54 W would be 34% and 33%, respectively.

In conclusion, we have demonstrated, for the first time, to the best of our knowledge, a side-pumped Nd:YLF laser system emitting in the 1.3 μm region. A diffraction-limited laser beam with a maximum output power of 14.9 W at 1313 nm is obtained with 54 W of absorbed pump power. This represents 27.7% optical efficiency and 45% slope efficiency. We analyzed the effect of the spectral broadening of the pump laser on laser efficiency. With a pump diode of less than 2.8 nm FWHM linewidth, DBMC technology could be capable of delivering a record optical-to-optical efficiency of 34% when pumped at 792 nm in a simple and compact cavity setup.

This study was funded by FAPESP (grant no. 2012/11437-8) and CNPq (grant no. 2012/470413).

References

1. D. F. T. Silva, R. A. Mesquita-Ferrari, K. P. S. Fernandes, M. P. Raelle, N. U. Wetter, and A. M. Deana, *Photochem. Photobiol.* **88**, 1211 (2012).
2. S. Parker, *Br. Dent. J.* **202**, 73 (2007).
3. J. T. Murray, R. C. Powell, N. Peyghambarian, D. Smith, W. Austin, and R. A. Stolzenberger, *Opt. Lett.* **20**, 1017 (1995).
4. P. Laporta, S. Longhi, S. Taccheo, O. Svelto, and G. Sacchi, *Opt. Lett.* **18**, 31 (1993).
5. J. Lu, J. Lu, T. Murai, K. Takaichi, T. Uematsu, J. Xu, K. Ueda, H. Yagi, T. Yanagitani, and A. A. Kaminskii, *Opt. Lett.* **27**, 1120 (2002).
6. J. Saikawa, Y. Sato, T. Taira, O. Nakamura, and Y. Furukawa, presented at Advanced Solid-State Photonics Conference (2005), paper 1L.
7. Y. Yan, H. Zhang, Y. Liu, X. Yu, H. Zhang, J. He, and J. Xin, *Opt. Lett.* **34**, 2105 (2009).
8. A. M. Deana, I. M. Ranieri, S. L. Baldochi, and N. U. Wetter, *Appl. Phys. B* **106**, 877 (2012).
9. H. Vanherzeele, *Opt. Lett.* **13**, 369 (1988).
10. Y. F. Lü, J. Xia, X. H. Zhang, A. F. Zhang, J. G. Wang, L. Bao, and X. D. Yin, *Appl. Phys. B* **98**, 305 (2010).
11. Y. Wei, S. Xu, C. H. Huang, F. J. Zhuang, W. D. Chen, L. X. Huang, X. L. Wang, and G. Zhang, *Laser Phys.* **22**, 1029 (2012).
12. C. L. Li, X. H. Zhang, W. Liang, and Z. M. Zhao, *Laser Phys.* **21**, 340 (2011).
13. A. M. Deana, E. C. Sousa, I. M. Ranieri, S. L. Baldochi, and N. U. Wetter, *Proc. SPIE* **8235**, 82350G (2012).
14. N. U. Wetter, F. A. Camargo, and E. C. Sousa, *J. Opt. A* **10**, 104012 (2008).
15. N. U. Wetter, E. C. Sousa, F. A. Camargo, I. M. Ranieri, and S. L. Baldochi, *J. Opt. A* **10**, 104013 (2008).
16. N. U. Wetter and A. M. Deana, *Laser Phys. Lett.* **10**, 035807 (2013).
17. A. Minassian, B. Thompson, and M. J. Damzen, *Appl. Phys. B* **76**, 341 (2003).
18. N. U. Wetter, E. C. Sousa, I. M. Ranieri, and S. L. Baldochi, *Opt. Lett.* **34**, 292 (2009).
19. J. Harrison, P. F. Moulton, and G. A. Scott, in *Conference on Lasers and Electro-Optics* (1995), postdeadline paper CPD-20.
20. A. M. Deana and N. U. Wetter, *Proc. SPIE* **8433**, 84330B (2012).